Zinc and manganese redox potentials in organic solvents and their influence on nickel-catalyzed cross-electrophile coupling

Authors: Zhi-Ming Su,[1] Ruohan Deng,[1] Shannon S. Stahl[1]*

[1]Department of Chemistry, University of Wisconsin-Madison, 1101 University Avenue, Madison, WI 53706, USA.

* Correspondence to: stahl@chem.wisc.edu

Abstract:

Zinc and manganese are widely used as reductants in synthetic methods, such as nickel-catalyzed cross-electrophile coupling (XEC) reactions, but their redox potentials are unknown in organic solvents. Here, we show how open-circuit potential measurements may be used to determine the thermodynamic potentials of Zn and Mn in different organic solvents and in the presence of common reaction additives. The impact of these Zn and Mn potentials is analyzed for a pair of Ni-catalyzed reactions, each showing a preference for one of the two reductants. Ni-catalyzed coupling of *N*-alkyl-2,4,6-triphenylpyridinium reagents (Katritzky salts) with aryl halides are then compared under chemical reaction conditions, using Zn or Mn reductants, and under electrochemical conditions, performed at applied potentials corresponding to the Zn and Mn reduction potentials and at potentials optimized to achieve the maximum yield. The collective results illuminate the important role of reductant redox potential in Ni-catalyzed XEC reactions.

Transition metal-catalyzed coupling reactions are the predominant methods for carbon-carbon bond formation in synthetic chemistry. [1–3] Ni-catalyzed cross-electrophile coupling (XEC) reactions have been the focus of growing development and application, motivated by their use of non-precious-metal catalysts and access to more diverse and lower-cost reagents relative to reactions that employ organometallic nucleophiles as coupling partners (**Fig. 1A**).[4–8] Initial applications developed in the 1990s featured aryl halides and activated alkyl halides as coupling partners,[9–12] but the available methods have expanded significantly and now include an array of other synthetically useful substrates. [8,13–16]

Ni-catalyzed XEC reactions require a stoichiometric source of electrons to support the overall cross-coupling reaction, and electron transfer is featured in key steps in the catalytic mechanisms. For example, reduction of the Ni catalyst to low-valent intermediates is needed to initiate oxidative addition or halogen-atom transfer from the organic electrophiles. Various reductants have been used to promote these reactions,[17–28] but heterogeneous zinc or manganese metal powders are the most widely used.[8] The choice of Zn or Mn as the reductant can significantly impact the reaction outcome. This behavior is illustrated by two representative XEC reactions reported recently by Shu and coworkers (**Fig. 1B**).[29,30] In the first example, cross-coupling of a vinyl acetate and an alkyl bromide proceeds effectively with Zn, but not with Mn, as the reductant (93% and 18% yields, respectively).[29] The second example, which features cross-coupling of aryl triflates and benzylic alcohols activated *in situ* to generate benzyl oxalates, shows the opposite trend, with higher yields obtained with Mn rather than Zn (82% and 15% yields, respectively).[30] Observations could be qualitatively rationalized by the reduction potentials of Zn and Mn, relative to the redox potentials needed to promote individual steps in catalytic mechanisms with different Ni catalyst systems and/or substrates.[31–33] The thermodynamic potentials of Zn and Mn in organic solvents, however, are not known, and factors that influence their potentials under typical reaction conditions have not been explored.

The thermodynamic potentials and speciation of Zn and Mn are well defined in aqueous solution from pH 0-14, as depicted in their Pourbaix diagrams (**Fig. 1C**);[34,35] however, the potentials from these diagrams are not straightforwardly translated to organic solvents. The redox potentials for Zn and Mn, –0.76 and –1.18 V, respectively, versus the standard hydrogen electrode (SHE), are commonly cited in the XEC literature. In many cases, these values are adjusted by simple mathematical conversion from SHE

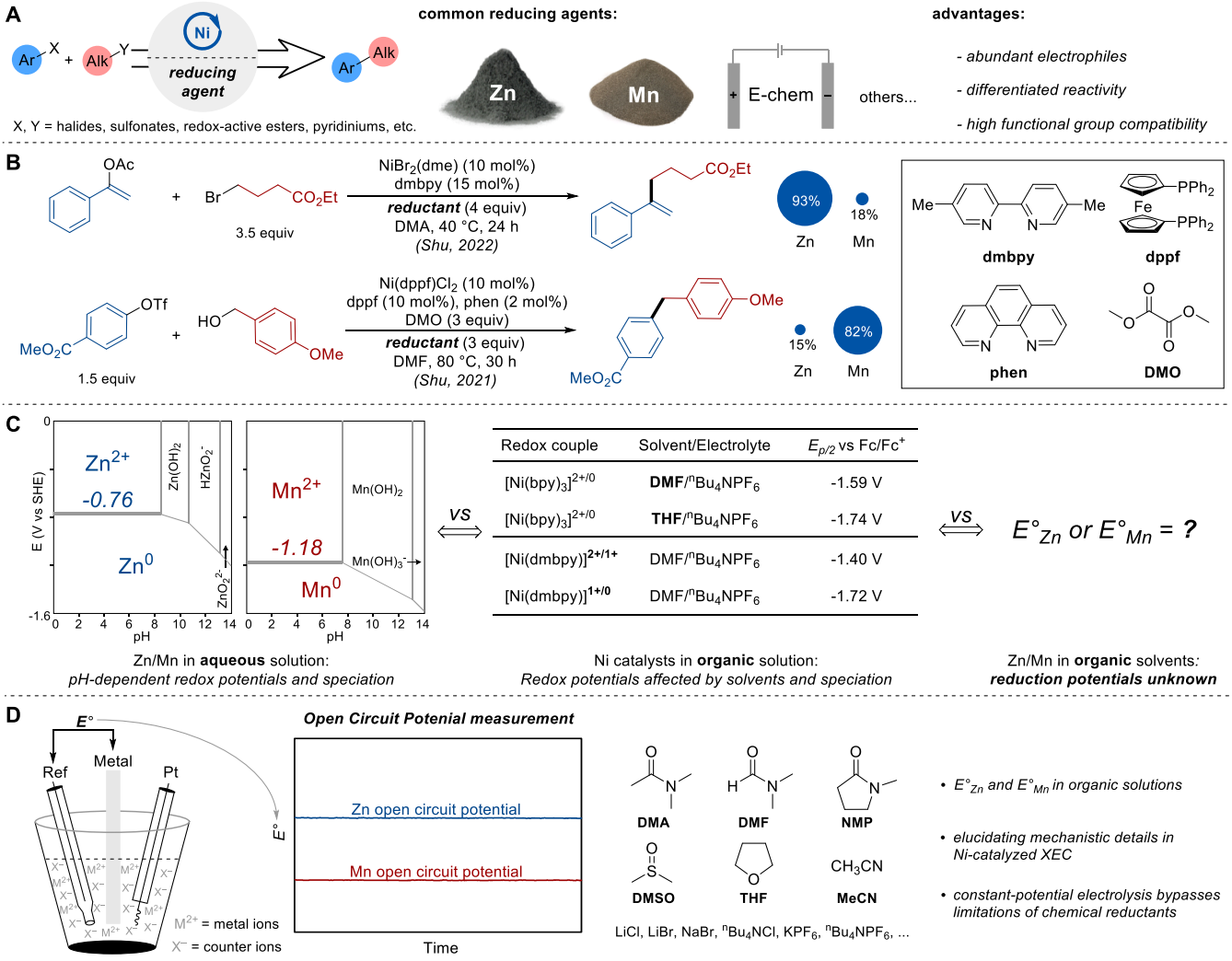

Fig. 1. Metal reductants in Ni-catalyzed XEC. (A) General depiction of Ni-catalyzed C(sp^2)–C(sp^3) cross-electrophile coupling (XEC) reactions. (B) Selected examples of Ni-catalyzed XEC reactions showing the impact of metal reductants on product yields. (C) Pourbaix diagrams for Zn and Mn in aqueous solution and selected redox potentials of Ni catalysts in organic solvent. (D) Schematic diagram illustrating open circuit potential measurement of thermodynamic potentials of metal reductants. Dme = 1,2-dimethoxyethane, bpy = 2,2′-bipyridine, dmbpy = 5,5′-dimethyl-2,2′-bipyridine, DMO = dimethyl oxalate, phen = 1,10-phenanthroline, dppf = 1,1′-bis(diphenylphosphino)ferrocene, SHE = standard hydrogen electrode, Fc/Fc^+ = ferrocene/ferrocenium.

to a reference electrode or reference potential used in an organic solvent, such as the saturated calomel electrode, SCE, or ferrocene/ferrocenium, Fc/Fc^+.[36] Values obtained by this approach are fraught with complications, however, as they fail to account for the influence of the solvent or reaction additives on the $Zn^{2+/0}$ and $Mn^{2+/0}$ potentials. The reductant redox potentials are especially important in relationship to redox potentials of the Ni^{II} catalyst, which can undergo one- or two-electron reduction steps depending

on the identity of the ancillary ligand (**Fig. 1C**). The identity of the solvent and additives also influences the Ni-based redox potential(s). Each of these considerations complicate fundamental understanding and systematic optimization of Ni-catalyzed XEC reactions that employ Zn and Mn reductants.

Here, we report open circuit potential measurements that provide direct analysis of the thermodynamic potentials of Zn and Mn reductants in organic solvents (**Fig. 1D**). The results reveal the impact of solvents and additives on the reduction potentials of heterogeneous metal reductants and enable direct comparison of these values with the potentials of substrates, catalysts, and other homogeneous redox-active species in organic reactions. The implications of these measurements are illustrated through a pair of studies that correlate the Zn and Mn reduction potentials with the product yields associated with these reductants and redox potentials of the Ni complexes used in the catalytic reactions. Finally, we analyze the XEC reaction of *N*-alkyl-2,4,6-triphenylpyridinium reagents (Katritzky salts) with aryl halides using Zn and Mn as heterogeneous reductants. The results are directly compared to the performance of these reactions with constant-potential electrolysis reactions conducted at variable potentials, including electrochemical potentials that match the thermodynamic potentials of Zn and Mn under the reaction conditions. The results of this analysis show how control over the reduction potential of a chemical reagent or an electrode has significant impact on the outcome of Ni-catalyzed XEC reactions.

Results and Discussion

Measurement of thermodynamic potentials of Zn and Mn

We initiated our study by measuring open circuit potentials (OCPs) for zinc and manganese relative to a reference electrode ($Ag/AgNO_3$) under a variety of conditions relevant to Ni-catalyzed XEC reactions (**Fig. 2A**). OCPs are obtained by using a potentiostat without passing current or applying an external voltage, and they represent thermodynamic potentials that are unaffected by electrochemical kinetics.[37,38] Six solvents commonly used in Ni-catalyzed XEC reactions were selected for OCP measurement to probe the influence of solvent on the Zn and Mn reduction potentials (**Fig. 2B**): dimethylformamide (DMF), dimethylacetamide (DMA), dimethyl sulfoxide (DMSO), N-methyl-2-pyrrolidone (NMP), acetonitrile (MeCN), and tetrahydrofuran (THF). Zn^{2+} or Mn^{2+} salts were included in the solution (10 mM) to ensure well-defined thermodynamic conditions for the redox process of interest (i.e., $M \rightleftharpoons M^{2+} + 2e^-$). The OCPs

measured in the different solvents were converted to formal potentials versus Fc/Fc^+ ($E°'$) by correcting for the non-standard-state concentration of the M^{2+} ions (see Section 2 of SI for details). The redox potential of $[Ni(bpy)_3]Cl_2$ was also measured in each of these solvents to provide a benchmark for Ni-based redox potentials (black data, **Fig. 2B**).

In amide solvents (DMF, DMA, and NMP), the Zn reduction potential is nearly constant (–1.36 V, –1.35 V), while Mn shows modest variation (–1.52 ± 0.04 V). The Zn and Mn potentials in DMSO are similar to the corresponding potentials observed in amide solvents ($\Delta E°' \leq 70$ mV). In contrast, the Zn and Mn potentials change substantially in MeCN and THF, increasing by up to 400–500 mV in MeCN relative to those measured in DMSO and amide solvents. The thermodynamic potentials of Zn and Mn are more positive than those of $[Ni(bpy)_3]Cl_2$, although the difference is rather small for Mn in DMSO and amide solvents ($\Delta E \leq 90$ mV). A somewhat larger difference is evident for Zn in these solvents ($\Delta E \leq 280$ mV).

The unique behavior of MeCN has important implications for Ni-catalyzed XEC reactions. The high reduction potentials observed for Zn and Mn in MeCN likely explain why XEC reactions are rarely conducted with these reductants in MeCN.[17,24] For example, Weix and coworkers evaluated a series of solvents, including MeCN, for the cross-coupling of benzyl chloride with phenyl iodide. Efficient cross-coupling was observed in DMA with Zn as the reductant, affording 82% yield of diphenylmethane, while only 15% yield was observed in MeCN (**Fig. 2C**).[24] This result could be rationalized by unfavorable thermodynamics for Zn reduction of the Ni catalyst in MeCN. Support for this hypothesis was obtained by conducting constant-potential electrolysis experiments in DMA and MeCN, applying potentials associated with the reduction potential of Zn in each solvent. At an applied potential of –0.93 V, the Zn reduction potential in MeCN, negligible current was observed in both solvents with >90% unreacted starting materials remained after 18 h. At the more reducing potential of –1.35 V, the Zn reduction potential in DMA, sustained current and moderate-to-good product yields were observed in both solvents (50% in DMA, 78% in MeCN; see full screening data in Supplementary Table 2). These observations show how solvent effects on the reduction potential of metallic reductants can have a significant influence on the outcome of reductive coupling reactions.

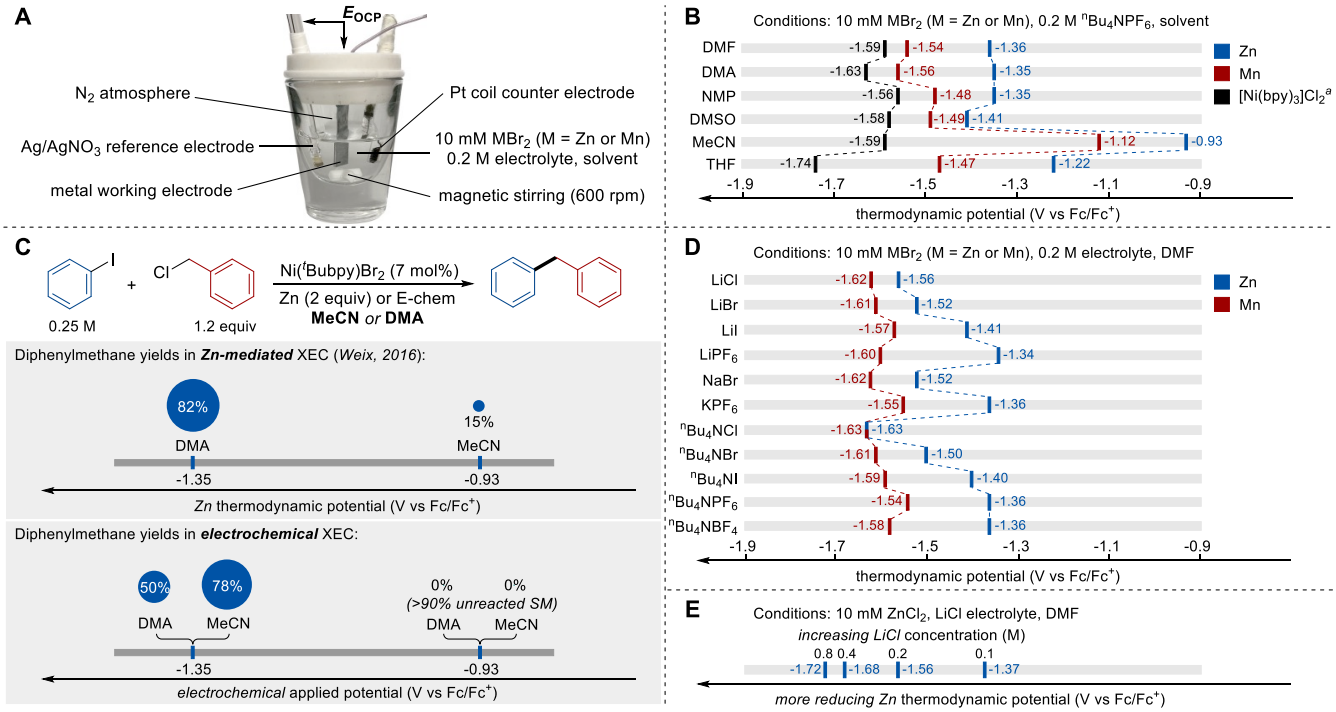

Fig. 2. **Thermodynamic potentials of Zn and Mn.** (A) Experimental set-up for open circuit potential measurements. (B) Solvent effects on thermodynamic potentials of Zn and Mn and the redox potential of $[Ni(bpy)_3]Cl_2$ (^{a} see Supplementary Fig. 5). (C) Comparison of the results of chemical and electrochemical Ni(^{t}Bubpy)Br_2-catalyzed coupling of benzyl chloride and phenyl iodide. (D) Additive effects on the thermodynamic potentials of Zn and Mn. (E) LiCl concentration effect on the thermodynamic potentials of Zn.

DMF is one of the most common solvents used for XEC reactions, and additives, such as LiCl, LiBr, among others, are often included in the reaction mixture. OCP measurements for Zn and Mn in the presence of various additives (200 mM) in DMF show that the Zn reduction potential can change by nearly 300 mV (**Fig. 2D**), depending on the additive identity. Only small variations were observed with Mn ($\Delta E \leq 100$ mV). Halide ions, especially chloride salts, shift the Zn reduction potential to more negative values relative to those recorded in the presence of weakly coordinating anions. With ^{n}Bu$_4$NCl, Zn has a reduction potential that matches Mn. As the quantity of these additives is commonly screened in the development of XEC reactions,[39,40]. OCP measurements were performed with different concentrations of LiCl. The data in **Fig. 2E** show that Zn becomes more reducing at higher LiCl concentration (ΔE = 350 mV from [LiCl] = 0.1– 0.8 M). These observations highlight a crucial role of halide ions in XEC reactions. For example, LiCl has been reported to accelerate Ni-catalyzed XEC reactions, and this behavior was attributed to the kinetic influence of chloride and/or lithium ions on Ni^{II} reduction by Zn metal.[41] The

results in **Fig. 2**, however, show that Zn is a stronger reductant in the presence of LiCl, highlighting an important, but previously unrecognized, thermodynamic contribution to this reaction.

Analyzing the preference for Zn or Mn reductants in Ni-catalyzed XEC reactions.

The preferred reductant in Ni-catalyzed XEC reactions can vary between Zn and Mn. The reduction potentials measured for these metals together with redox potentials of the Ni catalysts used in the reactions provide a foundation for understanding the origin of the preferred reductant. We elected to explore this approach using two reactions reported by Shu and coworkers depicted in **Fig. 1B**. The cross-coupling of alkenyl acetates and alkyl bromides proceeds effectively with Zn, but not with Mn, as the reductant (**Fig. 3A**).[29] This reaction was proposed to be initiated by reduction of Ni^{II} to Ni^{I}, followed by coordination and oxidative addition of the alkenyl acetate to form an alkenyl-Ni^{III} species. One-electron reduction of this species to give an alkenyl-Ni^{II} species and reaction with an alkyl radical was then proposed to generate the desired product. The cross-coupling of benzyl alcohols with aryl triflates uses dimethyl oxalate (DMO) to convert the alcohol to an oxalic ester electrophile, and this reaction proceeds effectively with Mn, but not with Zn, as the reductant (**Fig. 3B**).[30] The reaction was proposed to be initiated by reduction of Ni^{II} to Ni^{0}, in this case, followed by reaction of Ni^{0} with the benzyl oxalate to afford a benzyl-Ni^{II} species. One-electron reduction of this species to give a benzyl-Ni^{I} and oxidative addition of aryl triflate was then proposed to afford the desired product.

Analysis of these reactions was initiated by recording CVs of the Ni catalysts in their corresponding reaction solvents (DMA, DMF). CVs were obtained in the presence and absence of alkenyl acetate or benzyl oxalate, the substrates proposed to initiate reaction with their respective catalysts (**Figs. 3C** and **3D**; see Supplementary Figs. 6 and 7 for CVs involving both coupling partners). For the first reaction, the CV of the Ni catalyst alone reveals two quasi-reversible redox couples, reflecting sequential one-electron reduction of Ni^{II}. In the presence of 10 equiv alkenyl acetate, a new reduction peak is evident at –1.29 V, more positive than the original $Ni^{II/I}$ feature and consistent with the proposed alkene complexation to Ni^{I}. In addition, increased current is observed for the peak at –1.46 V and, even more significantly, –1.73 V. The reduction potentials of Zn and Mn, determined from OCP measurements under the same conditions,

are –1.31 V (Zn) and –1.55 V (Mn). These data suggest that the preference for Zn as the reductant for this reaction reflects the ability of Zn to reduce Ni^{II} to Ni^{I} without significant generation of Ni^{0}. The reduction

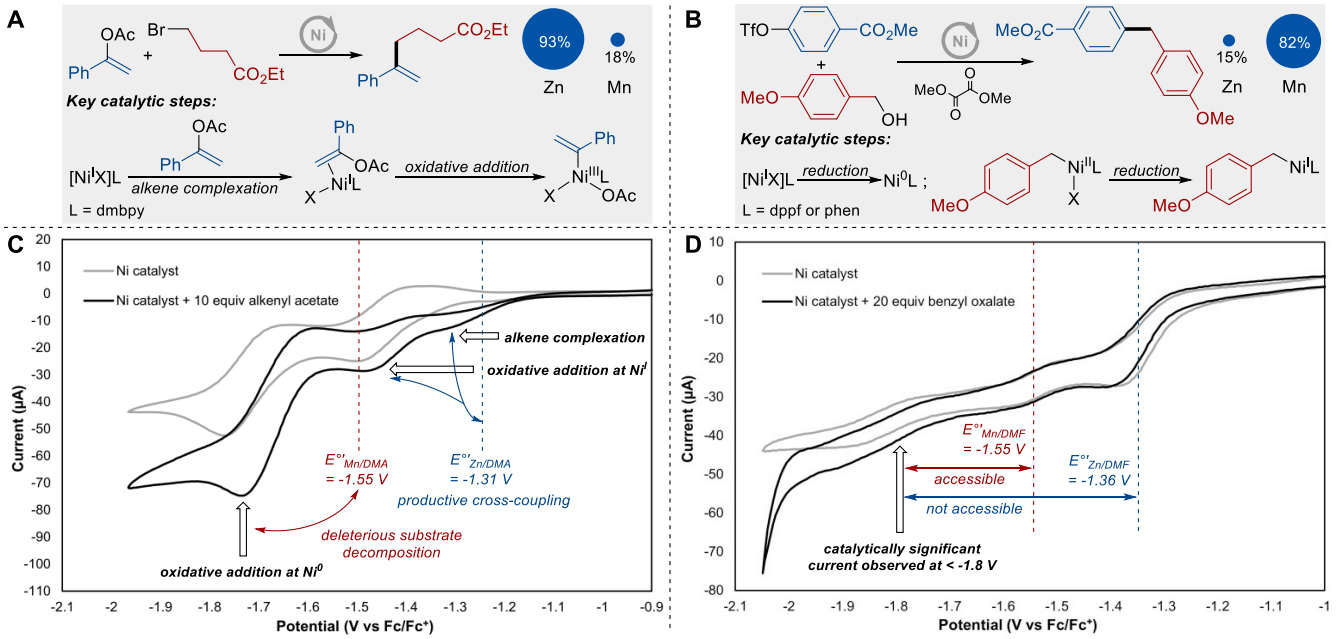

Fig. 3. Correlation of Zn and Mn thermodynamic potentials with Ni-based redox processes in Ni-catalyzed XEC. (A) Reductive cross-coupling of styrenyl acetate with an alkyl bromide using a Ni/dmbpy catalyst (dmbpy = 5,5′-dimethyl-2,2′-bipyridine). (B) The net cross-coupling of benzyl alcohol with aryl triflate using dimethyl oxalate to activate the alcohol using a Ni/mixed-ligand catalyst system (ligands: phen = 1,10-phenanthroline, dppf = 1,1′-bis(diphenylphosphino)ferrocene). (C) CV analysis of Ni/dmbpy in the absence and presence of the substrate. (D) CV analysis of Ni/dppf/phen in the absence and presence of the substrate.

potential of Mn is sufficiently close to $Ni^{I/0}$ potential to generate Ni^{0}, which was shown to promote alkyl-alkyl and vinyl-vinyl homocoupling in addition to the formation of other side products.[29]

A similar approach was adopted to analyze the cross-coupling of benzyl alcohol and aryl triflate (**Fig. 3D**), using a benzyl oxalate directly as the coupling partner to facilitate the CV analysis. This reaction features two different ancillary ligands, dppf and phen (dppf = 1,1′-bis(diphenylphosphino)ferrocene; phen = 1,10-phenanthroline), and the CV trace of the Ni catalyst shows multiple reduction peaks. The first peak at –1.37 V is attributed to one-electron reduction of Ni^{II} to Ni^{I}, while assignments of the peaks at lower potentials, –1.56 V and –1.86 V, are complicated by the mixture of ligands present. Addition of benzyl oxalate (20 equiv) to the solution leads to a small increase in current at potentials lower than approximately –1.60 V, relative to the Ni-only CV. The reduction potentials of Zn (–1.36 V) and Mn (–1.55 V), determined by OCP measurements under these conditions, suggest that the preference for Mn as

the reductant for this reaction arises from the need to access the lower-potential Ni species in this reaction, unlike the first reaction, which leads to deleterious reactivity at lower potentials. These results, for the first time, show how redox potentials of metal reductants in organic solvents correlate with catalyst redox potentials in XEC reactions.

Comparison of Ni-catalyzed XEC reactions using chemical (Zn, Mn) and electrochemical reduction.

Metallic Zn and Mn are effective reductants for many reductive cross-coupling reactions, but their individual redox potentials are not necessarily optimal for every reaction, while electrochemical potentials can be tuned continuously over a wide range.[42] The OCP measurements outlined herein enable the first direct comparison of chemical and electrochemical Ni-catalyzed XEC reactions at reduction potentials of Zn and Mn under the reaction conditions, and these results may be compared with electrochemical reactions conducted at other applied potentials. Reactions with *N*-alkyl-2,4,6-triphenylpyridinium reagents (Katritzky salts)[32,43–46] represent a compelling target for exploration of these issues because they exhibit variable performance in Ni-catalyzed XEC reactions when using homogenous organic reductants with different reduction potentials.[26]

Two Katritzky salts, one with a 1° alkyl and one with a 2° alkyl substituent (**1** and **2**, respectively), were investigated in XEC reactions with six different (hetero)aryl bromides (**Fig. 4**). Previously reported thermochemical conditions using Mn as the reductant[44] were adapted to electrochemical coupling of **1** and **2** with ethyl 4-bromobenzoate (see Supplementary Table 3 for evaluation of different cell configurations, electrode materials, electrolytes, and reaction temperatures). Good results were observed under constant potential conditions in an undivided cell with a Ni foam cathode and sacrificial Fe anode. The 1° Katritzky salt **1** performed best at 60 °C, while the more reactive 2° Katritzky salt **2** led to higher yields at room temperature (Conditions **A** and **B**, **Fig. 4**). Each pair of substrates was then compared under four reaction conditions: two thermochemical conditions using metallic Zn and Mn powder as the reductant, and two electrochemical conditions conducted at applied potentials corresponding to $E^{\circ\prime}_{Zn}$ (–1.31 V) and $E^{\circ\prime}_{Mn}$ (–1.55 V) determined from OCP measurements with Zn and Mn under the reaction conditions. A fifth condition was then used for each substrate pair, based on optimization of the applied potential.

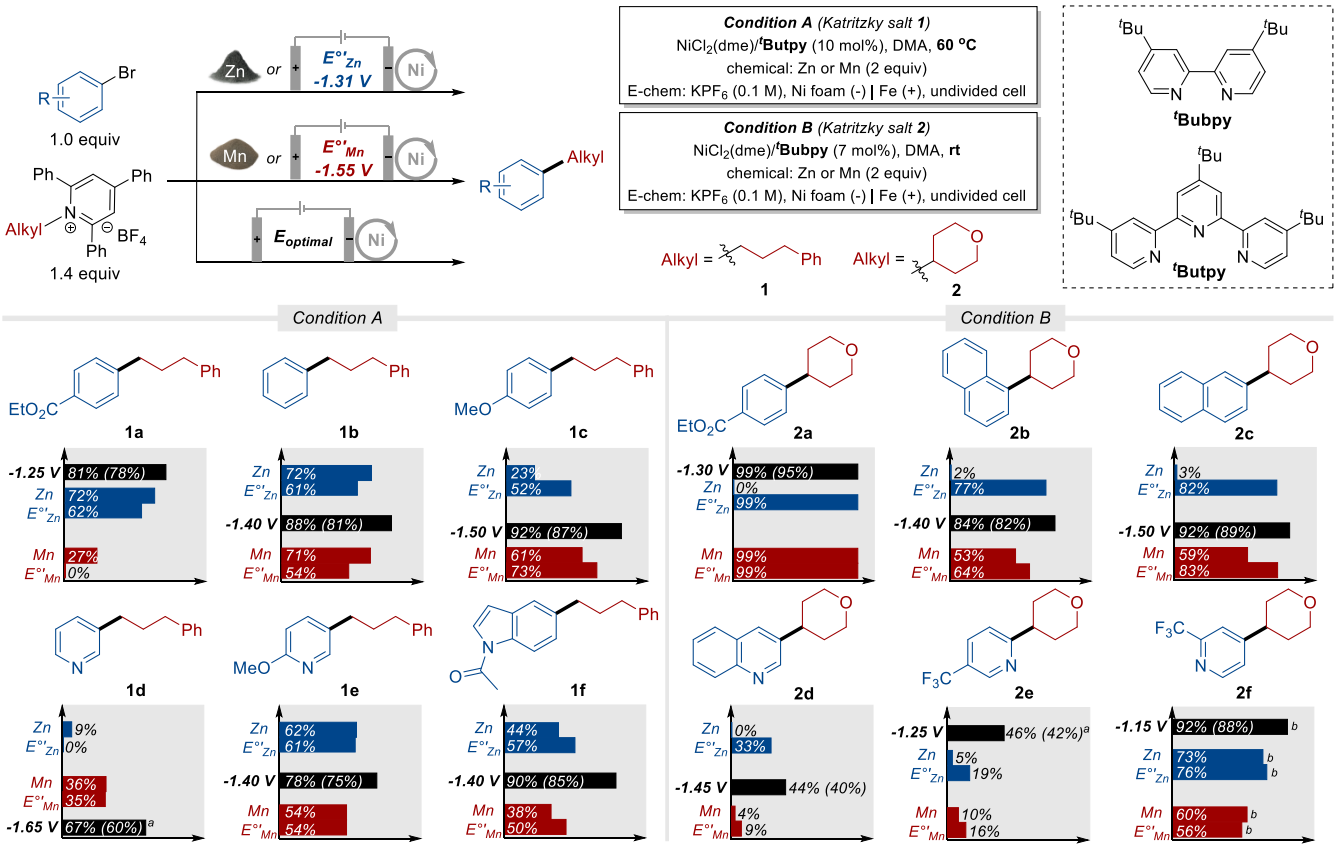

Fig. 4. Cross-electrophile coupling reactions of alkyl Katritzky salts with aryl bromides. Reactions were conducted thermochemically with Zn or Mn as the reductant, or electrochemically at varied applied potential. See the Supplementary Information for full experimental details. Yields determined by ^{1}H NMR spectroscopy; isolated yields are shown in parentheses. [a] LiBr (2 equiv) instead of KPF_6. [b] Aryl chloride was used instead of aryl bromide.

The data in **Fig. 4** show how thermochemical and electrochemical reduction methods perform at the same potential ($E^{\circ\prime}_{Zn}$ and $E^{\circ\prime}_{Mn}$). For example, coupling product **1a** was obtained in 72% yield with Zn and a 62% yield under electrochemical conditions at the Zn potential (–1.31 V). Significantly lower yields were observed with Mn (27%) and under electrochemical conditions at the Mn potential (0%; –1.55 V). Quantitative differences between chemical and thermochemical conditions can arise from various factors, for example, differences in the mass transport behavior of dissolved species interacting with suspended metal particles versus a solid-state electrode, and differences in the redox-active surface area of the metal powders and electrodes, that could alter the outcome. Nonetheless, the results in **Fig. 4** show good qualitative agreement between thermochemical and electrochemical results obtained at the Zn potential of substrates **1a–f** and **2f**, and at the Mn potential for all substrates. Notable differences were observed for many of the XEC reactions of **2** at the Zn potential: negligible quantities of **2a–e** were observed under

these conditions, while the corresponding electrochemical conditions (at $E^{\circ\prime}_{Zn}$) led to moderate-to-good product yields. Further analysis of this behavior showed that soluble Zn^{II} salts, generated in the reactions that used metallic Zn, convert the aryl bromide into the proto-dehalogenation byproduct, likely via the formation of protolytically sensitive arylzinc species (see Supplementary Table 4).[40,47]

The reactions of each substrate pair were then evaluated at different applied potentials, and the results showed that higher yields could be obtained at potentials other than $E^{\circ\prime}_{Zn}$ or $E^{\circ\prime}_{Mn}$ in all cases. For example, **1a** was generated in 81% yield at –1.25 V, a redox potential higher than $E^{\circ\prime}_{Zn}$ and $E^{\circ\prime}_{Mn}$. A survey of the results shows that the optimal potential changes for each reaction, and even the position of the optimal potentials relative to the Zn and Mn potentials changes. For the six reactions performed with the 1° Katritzky salt **1**, only **1a** performs best at a potential higher than $E^{\circ\prime}_{Zn}$. Four products (**1b**, **1c**, **1e**, **1f**) exhibit an optimal yield at a potential between Zn and Mn, and one (**1d**) maximizes at a potential more negative than $E^{\circ\prime}_{Mn}$ (**Fig. 4**). With the 2° Katritzky salt **2**, three of the products afford the highest yields at a potential higher than $E^{\circ\prime}_{Zn}$ (**2a**, **2e**, **2f**), while three are optimal at potentials between Zn and Mn (**2b**, **2c**, **2d**).

The results in **Fig. 4** have important implications for Ni-catalyzed XEC reactions. Large-scale applications of these reactions with chemical reductants are already complicated by challenges in using metal-powder reagents (non-uniform particle properties/reactivity, difficulty in suspending dense powders in reactors[48]) or air-sensitive organic reductants[28]. The data in **Fig. 4** show that the quantized/non-tunable redox potentials of chemical reagents will limit opportunities to optimize the reaction performance. Each of these challenges may be addressed by using electrochemistry to supply the electrons needed in the reaction.

Conclusion

The results outlined above document thermodynamic potentials of Zn and Mn reductants in organic solutions for the first time, revealing the influence of different solvents and additives on the reduction potentials. These data are ideally paired with cyclic voltammetry studies to gain fundamental insights into the relationship between the redox potential of the reductant and catalytic species and intermediates in the reaction. The approach used here is readily adapted to other reduction and reductive coupling reactions,

including those using different metal reductants, solvents, and reaction conditions. Access to the Zn and Mn reduction potentials also provided the first opportunity to directly compare the influence of chemical versus electrochemical reduction methods on the reaction outcome. Good qualitative agreement is observed from reactions conducted at the same potential (e.g., at $E^{\circ\prime}_{Zn}$ or $E^{\circ\prime}_{Mn}$), but the optimization studies show that the optimal reduction potential is often different from the specific potentials accessible from the chemical reductants. These results highlight the importance of tuning the reductant redox potential when optimizing Ni-catalyzed XEC, and presumably other reductive coupling, reactions. The tunability of electrochemistry should offer significant advantages in the future development of these reactions.

Acknowledgements

Financial support for this work was provided by the NSF (CHE-2154698; thermodynamic potential measurements) and NIH (R35 GM134929; synthetic methodology studies). Spectroscopic instrumentation was supported by a generous gift from Paul J. and Margaret M. Bender, the NIH (S10 OD020022), and the NSF (CHE-1048642).

Author contributions

S.S.S. and Z.-M.S. conceived the project and designed the experiments. Z.-M.S. conducted all the experiments. R.D. contributed partially to electrochemical analysis and product purification. S.S.S. and Z.-M.S. wrote the manuscript.

Supplementary information

Supplementary Figs. 1–7, Supplementary Tables 1–4, experimental procedures, discussions, characterization data, and NMR spectra.

References

1. Corbet, J.-P. & Mignani, G. Selected Patented Cross-Coupling Reaction Technologies. *Chem. Rev.* **106**, 2651–2710 (2006).
2. Boström, J., Brown, D. G., Young, R. J. & Keserü, G. M. Expanding the medicinal chemistry synthetic toolbox. *Nat Rev Drug Discov* **17**, 709–727 (2018).
3. Buskes, M. J. & Blanco, M.-J. Impact of Cross-Coupling Reactions in Drug Discovery and Development. *Molecules* **25**, 3493 (2020).
4. Moragas, T., Correa, A. & Martin, R. Metal-Catalyzed Reductive Coupling Reactions of Organic Halides with Carbonyl-Type Compounds. *Chem. Eur. J.* **20**, 8242–8258 (2014).
5. Weix, D. J. Methods and Mechanisms for Cross-Electrophile Coupling of Csp^2 Halides with Alkyl Electrophiles. *Acc. Chem. Res.* **48**, 1767–1775 (2015).
6. Wang, X., Dai, Y. & Gong, H. Nickel-Catalyzed Reductive Couplings. in *Ni- and Fe-Based Cross-Coupling Reactions* (ed. Correa, A.) 61–89 (Springer International Publishing, 2017).
7. Richmond, E. & Moran, J. Recent Advances in Nickel Catalysis Enabled by Stoichiometric Metallic Reducing Agents. *Synthesis* **50**, 499–513 (2018).
8. Goldfogel, M. J., Huang, L. & Weix, D. J. Cross-Electrophile Coupling. in *Nickel Catalysis in Organic Synthesis* 183–222 (John Wiley & Sons, Ltd, 2020).
9. Chaussard, J. *et al.* Use of Sacrificial Anodes in Electrochemical Functionalization of Organic Halides. *Synthesis* **1990**, 369–381 (1990).
10. Durandetti, M., Nédélec, J.-Y. & Périchon, J. Nickel-Catalyzed Direct Electrochemical Cross-Coupling between Aryl Halides and Activated Alkyl Halides. *J. Org. Chem.* **61**, 1748–1755 (1996).
11. Durandetti, M., Périchon, J. & Nédélec, J.-Y. Asymmetric Induction in the Electrochemical Cross-Coupling of Aryl Halides with α-Chloropropionic Acid Derivatives Catalyzed by Nickel Complexes. *J. Org. Chem.* **62**, 7914–7915 (1997).
12. Durandetti, M., Gosmini, C. & Périchon, J. Ni-catalyzed activation of α-chloroesters: a simple method for the synthesis of α-arylesters and β-hydroxyesters. *Tetrahedron* **63**, 1146–1153 (2007).
13. Everson, D. A., Jones, B. A. & Weix, D. J. Replacing Conventional Carbon Nucleophiles with Electrophiles: Nickel-Catalyzed Reductive Alkylation of Aryl Bromides and Chlorides. *J. Am. Chem. Soc.* **134**, 6146–6159 (2012).
14. Rosen, B. M. *et al.* Nickel-Catalyzed Cross-Couplings Involving Carbon−Oxygen Bonds. *Chem. Rev.* **111**, 1346–1416 (2011).
15. He, F.-S., Ye, S. & Wu, J. Recent Advances in Pyridinium Salts as Radical Reservoirs in Organic Synthesis. *ACS Catal.* **9**, 8943–8960 (2019).
16. Karmakar, S., Silamkoti, A., Meanwell, N. A., Mathur, A. & Gupta, A. K. Utilization of C(sp^3)-Carboxylic Acids and Their Redox-Active Esters in Decarboxylative Carbon−Carbon Bond Formation. *Adv. Syn. Catal.* **363**, 3693–3736 (2021).
17. Perkins, R. J., Hughes, A. J., Weix, D. J. & Hansen, E. C. Metal-Reductant-Free Electrochemical Nickel-Catalyzed Couplings of Aryl and Alkyl Bromides in Acetonitrile. *Org. Process Res. Dev.* **23**, 1746–1751 (2019).
18. Hamby, T. B., LaLama, M. J. & Sevov, C. S. Controlling Ni redox states by dynamic ligand exchange for electroreductive Csp^3–Csp^2 coupling. *Science* **376**, 410–416 (2022).
19. Zhang, B. *et al.* Ni-electrocatalytic Csp^3–Csp^3 doubly decarboxylative coupling. *Nature* **606**, 313–318 (2022).

20. Franke, M. C. *et al.* Zinc-free, Scalable Reductive Cross-Electrophile Coupling Driven by Electrochemistry in an Undivided Cell. *ACS Catal.* **12**, 12617–12626 (2022).
21. Su, Z.-M. *et al.* Ni- and Ni/Pd-Catalyzed Reductive Coupling of Lignin-Derived Aromatics to Access Biobased Plasticizers. *ACS Cent. Sci.* **9**, 159–165 (2023).
22. Twilton, J. *et al.* Quinone-mediated hydrogen anode for non-aqueous reductive electrosynthesis. *Nature* **623**, 71–76 (2023).
23. Zhang, G., Xie, Y., Wang, Z., Liu, Y. & Huang, H. Diboron as a reductant for nickel-catalyzed reductive coupling: rational design and mechanistic studies. *Chem. Commun.* **51**, 1850–1853 (2015).
24. Anka-Lufford, L. L., Huihui, K. M. M., Gower, N. J., Ackerman, L. K. G. & Weix, D. J. Nickel-Catalyzed Cross-Electrophile Coupling with Organic Reductants in Non-Amide Solvents. *Chem. Eur. J.* **22**, 11564–11567 (2016).
25. Lv, L., Qiu, Z., Li, J., Liu, M. & Li, C.-J. N_2H_4 as traceless mediator for homo- and cross- aryl coupling. *Nat. Commun.* **9**, 4739 (2018).
26. Charboneau, D. J. *et al.* Tunable and Practical Homogeneous Organic Reductants for Cross-Electrophile Coupling. *J. Am. Chem. Soc.* **143**, 21024–21036 (2021).
27. Fu, H. *et al.* An asymmetric sp^3–sp^3 cross-electrophile coupling using 'ene'-reductases. *Nature* **610**, 302–307 (2022).
28. Charboneau, D. J., Hazari, N., Huang, H., Uehling, M. R. & Zultanski, S. L. Homogeneous Organic Electron Donors in Nickel-Catalyzed Reductive Transformations. *J. Org. Chem.* **87**, 7589–7609 (2022).
29. He, R.-D. *et al.* Reductive Alkylation of Alkenyl Acetates with Alkyl Bromides by Nickel Catalysis. *Angew. Chem. Int. Ed.* **61**, e202114556 (2022).
30. Guo, P. *et al.* Dynamic Kinetic Cross-Electrophile Arylation of Benzyl Alcohols by Nickel Catalysis. *J. Am. Chem. Soc.* **143**, 513–523 (2021).
31. Lin, Q. & Diao, T. Mechanism of Ni-Catalyzed Reductive 1,2-Dicarbofunctionalization of Alkenes. *J. Am. Chem. Soc.* **141**, 17937–17948 (2019).
32. Martin-Montero, R., Yatham, V. R., Yin, H., Davies, J. & Martin, R. Ni-catalyzed Reductive Deaminative Arylation at sp^3 Carbon Centers. *Org. Lett.* **21**, 2947–2951 (2019).
33. Day, C. S. *et al.* Elucidating electron-transfer events in polypyridine nickel complexes for reductive coupling reactions. *Nat. Catal.* **6**, 1–10 (2023).
34. Pourbaix, M. *Atlas of electrochemical equilibria in aqueous solutions*. *2nd ed*. (National Association of Corrosion Engineers, 1974).
35. Yu, Y. *et al.* High-Voltage Rechargeable Aqueous Zinc-Based Batteries: Latest Progress and Future Perspectives. *Small Sci.* **1**, 2000066 (2021).
36. Pavlishchuk, V. V. & Addison, A. W. Conversion constants for redox potentials measured versus different reference electrodes in acetonitrile solutions at 25°C. *Inorganica Chim. Acta* **298**, 97–102 (2000).
37. Kissinger, P. & Heineman, W. R. *Laboratory Techniques in Electroanalytical Chemistry, Revised and Expanded*. (CRC Press, 2018).
38. Elgrishi, N. *et al.* A Practical Beginner's Guide to Cyclic Voltammetry. *J. Chem. Educ.* **95**, 197–206 (2018).
39. Mirabi, B., Marchese, A. D. & Lautens, M. Nickel-Catalyzed Reductive Cross-Coupling of Heteroaryl Chlorides and Aryl Chlorides. *ACS Catal.* **11**, 12785–12793 (2021)

40. Kang, K., Huang, L. & Weix, D. J. Sulfonate Versus Sulfonate: Nickel and Palladium Multimetallic Cross-Electrophile Coupling of Aryl Triflates with Aryl Tosylates. *J. Am. Chem. Soc.* **142**, 10634–10640 (2020).
41. Huang, L., Ackerman, L. K. G., Kang, K., Parsons, A. M. & Weix, D. J. LiCl-Accelerated Multimetallic Cross-Coupling of Aryl Chlorides with Aryl Triflates. *J. Am. Chem. Soc.* **141**, 10978–10983 (2019).
42. Rafiee, M., Mayer, M. N., Punchihewa, B. T. & Mumau, M. R. Constant Potential and Constant Current Electrolysis: An Introduction and Comparison of Different Techniques for Organic Electrosynthesis. *J. Org. Chem.* **86**, 15866–15874 (2021).
43. Ni, S. *et al.* Ni-catalyzed deaminative cross-electrophile coupling of Katritzky salts with halides via C─N bond activation. *Sci. Adv.* **5**, eaaw9516 (2019).
44. Yue, H. *et al.* Nickel-catalyzed C–N bond activation: activated primary amines as alkylating reagents in reductive cross-coupling. *Chem. Sci.* **10**, 4430–4435 (2019).
45. Liao, J. *et al.* Deaminative Reductive Cross-Electrophile Couplings of Alkylpyridinium Salts and Aryl Bromides. *Org. Lett.* **21**, 2941–2946 (2019).
46. Twitty, J. C. *et al.* Diversifying Amino Acids and Peptides via Deaminative Reductive Cross-Couplings Leveraging High-Throughput Experimentation. *J. Am. Chem. Soc.* **145**, 5684–5695 (2023).
47. Klein, P., Lechner, V. D., Schimmel, T. & Hintermann, L. Generation of Organozinc Reagents by Nickel Diazadiene Complex Catalyzed Zinc Insertion into Aryl Sulfonates. *Chem. Eur. J.* **26**, 176–180 (2020).
48. Nimmagadda, S. K.; Korapati, S.; Dasgupta, D.; Malik, N. A.; Vinodini, A.; Gangu, A. S.; Kalidindi, S.; Maity, P.; Bondigela, S. S.; Venu, A.; Gallagher, W. P.; Aytar, S.; González-Bobes, F.; Vaidyanathan, R. Development and Execution of an Ni(II)-Catalyzed Reductive Cross-Coupling of Substituted 2-Chloropyridine and Ethyl 3-Chloropropanoate. *Org. Process Res. Dev.* **24**, 1141–1148 (2020).